Hadley Centre Technical Note 94

Real-time forcast skill for Europe in the combined Met Office and ECMWF monthly prediction system

July 2013

Bernd Becker, Emily Wallace, Andrew Williams, Alberto Arribas, Met Office.

"Real-time forecast skill for Europe in the combined Met Office and ECWMF monthly prediction system."

Bernd Becker, Emily Wallace, Andrew Williams, Alberto Arribas, Met Office.

Abstract:
Ensemble prediction systems for monthly-range forecasts attempt to account for uncertainty in numerical weather prediction (NWP) by sampling the distribution function of future atmospheric states. Forecast uncertainty derives from uncertainty in both the analysed initial conditions (analysis errors) and in the forecast evolution (model errors). Current operational systems are based on sampling the analysis errors through initial-condition perturbations and model errors through stochastic perturbations to parameterised model physics. One approach to improve sampling of model errors and also to widening the sampling of analysis errors, is to include more than one NWP model, and more than one operational analysis to which perturbations are added, in the ensemble system. Previous work on medium range time scales (10 days) has demonstrated from a small number of case-studies that this multi-model ensemble (MME) approach can perform significantly better than a single-model system such as the Ensemble Prediction System (EPS) run by the ECMWF (European Centre for Medium-Range Weather Forecasts). In this study a MME was created by combining the ECMWF monthly ensemble with the Met Office monthly ensemble, and was run weekly for a year to assess the benefits over a quasi-operational sample of forecasts. The results are compared with the operational ECMWF monthly prediction system. Results show that for probabilistic forecasts (assessed by relative operating characteristics) the MME has no significant forecast skill improvement relative to the monthly EPS. Recent findings in predictability research on the monthly timescale hint at improved forecast skill during active Madden-Julian-Oscillations. A composite analysis of the multi-model hindcast suggests a generic mechanism by that organized tropical convection influences the large scale synoptic pattern over Europe. Focussing on active MJO near initial conditions in real time forecasts yields statistically the same skill level as the MME.
These results are obtained with a pragmatic approach to combining a burst mode and a lagged mode initialized ensemble prediction system. It is found that the MME performs as well as the operational ECMWF monthly ensemble in this setup. ECMWF short range NWP forecast were used as pseudo observations in the verification. This is a questionable substitute for real observations. Such an incestuous data set may favour the ECMWF forecasting suite in the skill assessment. Results presented here therefore have to be viewed with caution.

1. Introduction

Monthly forecasting is difficult because the lead time is sufficiently long that much of the memory of the atmospheric initial conditions is lost (Buizza 1997) and it is too short for the slowly varying large scale boundary conditions of the ocean and land surface to exert a strong influence (Ma et al. 2013, Latif et al. 2006). For the time scales in between, wave responses induced by organized convection in the tropics may exert predictability affecting the mid latitudes and Europe (Blackburn et al. 2013, Moncrieff et al. 2007). Europe is a particularly difficult region to forecast due to high intrinsic variability at the exit of the polar jet and a fairly small land region with a complex coastline with shallow seas. Recent research (Cassou (2008), Lin and Brunet (2009)) has highlighted the Madden Julian Oscillation (MJO) as an important source of predictability for Europe at the sub-seasonal time range. The MJO is the dominant component of the intra seasonal (30-90 days) variability in the tropical atmosphere. It consists of large-scale coupled patterns in atmospheric circulation and deep convection that propagate eastward at a speed of ~5m/s through the tropical belt, initiating in the western hemisphere (phase 8/1) (Hendon, 2000), moving through the Indian Ocean (Phase 2/3) and Maritime Continent into the western Pacific warm pool region (Phase 4/5), eventually dissipating in the Pacific Ocean (Phase 6/7). The MJO can influence rainfall variability, the genesis of tropical cyclones and equatorial surface winds. Studies have linked the MJO to the NAO through atmospheric Rossby waves (Lin and Brunet, 2009). The MJO is an air-sea coupled oscillation (Hendon, 2000) and it can be accurately represented in forecast models only through atmosphere-ocean coupling (Woolnough et al. 2007). There is evidence (e.g. Fu et al., 2006) that the air-sea coupling extends the predictability of intra-seasonal oscillations into an extended forecast range of 2 to 4 weeks. Predictive skill may be increased during periods where the forecasting system responds to anomalous tropical heating realistically. The biggest impact of the MJO on the extra tropics has been shown for enhanced convection over the maritime continent (MJO phase 3/4) and for enhanced convection over the western hemisphere warm pool (MJO phase 6/7). The observed lagged association of the NAO and the MJO (Lin and Brunet, 2009) suggests the possibility that a medium- and extended-range forecast of the NAO and its associated weather will benefit from a good initial knowledge of the MJO phase. Therefore, it is important for an operational numerical prediction model to be able to simulate such an MJO–NAO connection.

The role of the MJO will be investigated by answering the question: "Does a multi-model ensemble improve skill in predictions over Europe on lead times beyond the medium range?" Multi-model ensemble (MME) techniques are known to be a useful and practical approach for minimising the effect on skill of inherent errors contained in individual models. Many forecast centres are actively engaging in operational monthly forecasts (CMC, JMA, Met Office, ECMWF, Canada, IRI)

because of successes in modelling slowly varying components of the climate system and their impact on weather, as well as the high demand for forecasts on such timescale.

A WMO initiative on sub-seasonal variability to investigate the usefulness/practicability of a monthly forecasting multi-model is being actively discussed (Anderson 2012). The jury is still out on the potential benefits from running a single ensemble versus a multi model ensemble on the monthly forecast time range.

Until recently, operational monthly forecasts at the Met Office (Becker 2004) were based on the ECMWF monthly forecast system (Vitart 2004). In 2009, the Met Office introduced an operational monthly forecast system integrated with its seasonal forecast system (Glosea4). This study investigates the potential benefits from combining the two forecasting systems.

The Met Office/ECMWF multi-model ensemble was run operationally for the period May 2011 to May 2012. This paper analyses hindcasts for both systems that are available for the period 1996 to 2009. The hindcast is used to investigate the response of the forecast systems over Europe to MJO events and also to define the model climatology for use in real-time forecasts. The forecasts (covering) are verified to assess the real-time skill of the multi-model. The remainder of this paper is organised as follows: the multi-model is described in Section 2; data sets used to assess the multi-model performance are described in Section 3, results from a composite analysis of the MJO in the model hindcasts and verification of real-time probabilistic quintile forecast, stratified by MJO activity is presented in Section 4, a discussion of the results is given in Section 5 and an outlook to further research is given in Section 6.

2. The multi-model ensemble prediction system

This section describes the ECMWF, the Met Office and the multi-model monthly forecast systems.

2.1. ECMWF system set up

The ECMWF monthly forecast system (MFS) is the extended Variational Ensemble Prediction system (VEPS) based on the Integrated Forecast System (IFS) (Pailleux 1997). The ECMWF forecast and hindcast are initialized in burst mode, which means that all ensemble members of one forecast share the same calendar dates for their initialization. A monthly ensemble forecast is produced every Thursday and every Monday. Only the Thursday forecast is accompanied with a matching hindcast and therefore the remainder of this study is concerned with the Thursday runs of the ECMWF monthly system only.

2.1.1. ECMWF forecast

The MFS consists of a 51-member ensemble of 32-day integrations. Each ensemble member is initialized from an analysis of the observed atmospheric state. To represent the uncertainty in initial conditions, flow-dependant perturbations are applied in regions of synoptic instability to initialise spread in the ensemble (Leutbecher et al., 2008). These perturbations are constructed using singular vectors which capture the fastest growing errors in the first 48 hours of the forecast (Buizza and Palmer 1995). Stochastic perturbations are also added during the model integration to account for uncertainty in parameterized physical processes (Palmer et al. 2009).

The first 10 days of the forecast are run with resolution T639 (30km) and 62 vertical levels. After day 10 the atmosphere is coupled to the ocean and model resolution is reduced to T399, equivalent to 60 km in mid latitudes. The ocean initial conditions at day 10 are taken from the last day of a 10-day ocean general circulation model integration, which is initialized from the ECMWF analysis (Balmaseda et al. 2008) and forced by the fluxes from the atmosphere-only integration. A detailed description of the VEPS system can be found in Vitart et al. (2008). During the period that we collected real-time monthly forecast, the IFS model cycle changed twice: the early part of the archive includes IFS model cycle CY36R4 coupled to the Hamburg Ocean Primitive Equation (HOPE) ocean model, on 18/05/2011 the IFS was upgraded to CY37R2 and on 17/11/2011 model cycle CY37R3 coupled to NEMO (Nucleus for European Modelling of the Ocean) was introduced. The impact of these changes is not investigated in this article.

2.1.2. ECMWF hindcast

Each forecast ensemble is accompanied by a set of hindcasts consisting of 5 ensemble members run for the same calendar period as the forecast but initialized for each of the most recent 18 years (1992 – 2010), forming a 90-member hindcast.

2.2. GloSea4 set up

Glosea4 is the operational Met Office monthly and seasonal ensemble prediction system. It is built around version 3 of the HadGEM family of models (Hewitt et al. 2010). The spatial resolution is N96L85 for atmosphere, which is approximately 135 km in the horizontal with 85 vertical levels, and tri-polar ORCA1L75 for ocean, in which the horizontal grid distance is 1 degree outside the tropics and 1/3 of a degree between 20S and 20N. The ocean model has 75 vertical levels. Further details of the GloSea4 configuration are given in Arribas et al. (2011).

2.2.1. GloSea4 forecast

Component models in Glosea4 are the UM (Met Office Unified Model) for the atmosphere, NEMO (Nucleus for European Modelling of the Ocean) for the ocean, CICE (Los Alamos sea ice model)

for sea ice, and MOSES (Met Office Surface Exchange Scheme) for land surface coupled through the OASIS coupler.

Four forecast ensemble members are produced daily. They share exactly the same initial conditions and differ only due to the stochastic kinetic energy backscatter scheme version 2 (SKEB2) (Tennant, 2011) in order to simulate model uncertainties. A lagged 28-member forecast ensemble is created by pulling together all forecasts available from the previous 7 dates every day.

2.2.2. GloSea4 hindcast

The 14-year fixed hindcast covers the 1996 to 2009. The ECMWF-interim reanalysis (ERA-interim) is used to initialize the atmosphere and land surface in the hindcast simulations following an anomaly initialization approach to avoid the inconsistency due to the different land surface schemes used in HadGEM3 and ERA-interim reanalysis. Land surface variables are calculated by adding ERA-interim anomalies to the HadGEM3 model climatology.

Ocean fields are initialized in the same way as in the forecast suite. The GloSea4 Ocean Data Assimilation (ODA) scheme consists of a parallel lower resolution version of the Met Office optimal interpolation scheme used for short-range ocean forecasting, except that atmospheric fluxes to force the ODA scheme are obtained from the ERA-interim rather than from the operational NWP system (Arribas et al. 2011) .

The hindcast period spans 14 years from 1996 to 2009. Initial dates are the 1st, 9th, 17th, and 25th of each month. Three ensemble members are generated for each initial hindcast date.

2.3. Deriving the Multi-Model

The ensemble initialization for the multi-model is described in Figure 1. For simplicity, we select forecasts from ECMWF (burst mode) and Glosea4 (lagged mode) valid at the same time. The ECMWF model is initialized on 00:00 GMT every Thursday. This date is chosen to be the central date in the middle of the time window from which the lagged Glosea4 ensemble members are selected, straddling the initial start date of the ECMWF. Some Glosea4 members have been initialized up to 3 days earlier; others are initialized up to three days after forecast Thursday. The lead time in the forecast period averages is always the same in the burst mode ECMWF ensemble but varies in the lagged Glosea4 ensemble. To estimate the model's climatological distribution at each forecast start date, the two closest hindcast start dates straddling the forecast date are chosen for the period 1996 to 2009, forming an 84 member hindcast for each forecast. All ECMWF data is interpolated (bi-linear) to the coarser resolution of the model used within Glosea4 (Hadgem3).

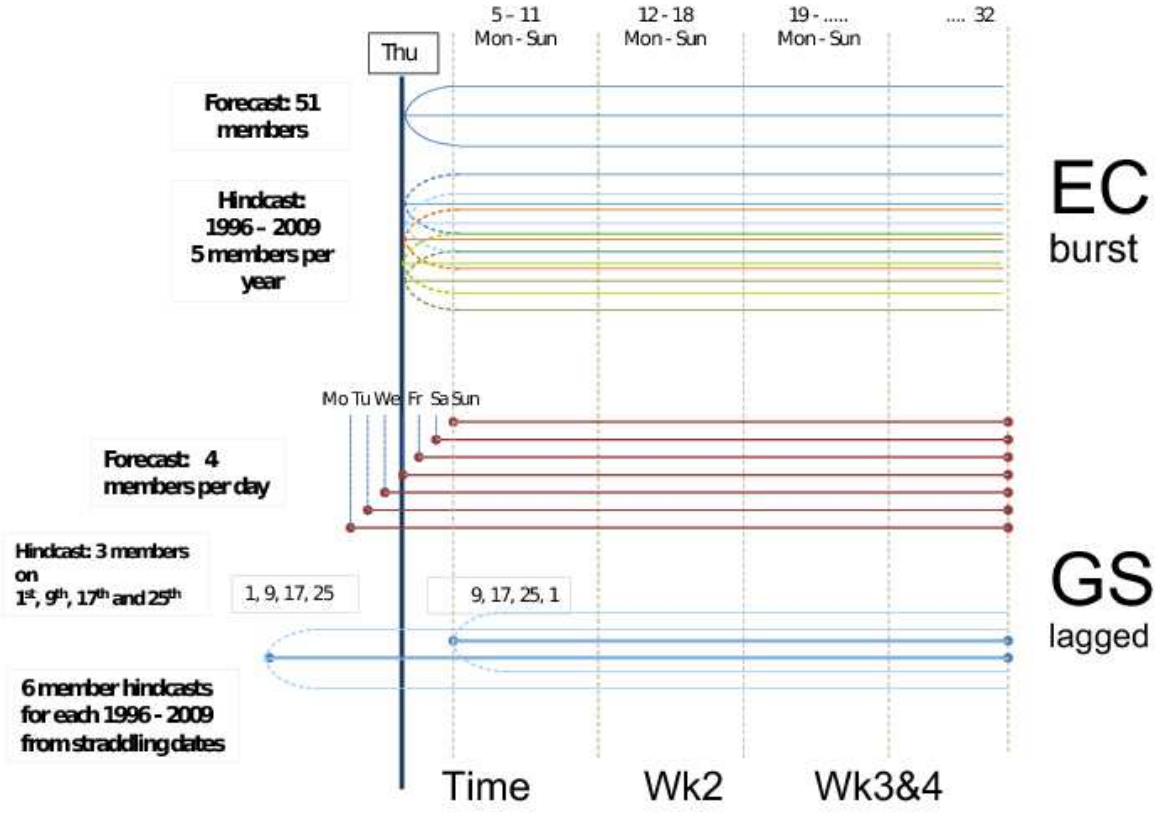

Figure 1: *The multi-model setup. Glosea4 ensemble members are combined with the ECMWF monthly forecast system once a week. The ECMWF monthly forecast system is shown on top. Fore– and Hindcast are initialized in burst mode. Each Thursday 51 forecast members are initialized from a perturbed initial state. For each of the past 18 years a five member hindcast is run. All hindcast and forecast members share the same systematic lead time dependant errors over the 32-day calendar period.*

Below, the lagged initialization approach of the Glosea model is shown. Four ensemble forecast members are produced every day. A 28-member forecast ensemble is created once a week by pulling together all forecasts from a 7 day window centred on the initial date of the burst mode ensemble.

A 14-year (1996-2009) Glosea Hindcast is initialised from ERA-interim and from ocean data reanalysis. Three members are produced on fixed start dates on the 1st, 9th, 17th, 25th of each month. A 84-member hindcast ensemble is created once a week by pulling together all hindcasts from the two start-dates straddling the initial date of the burst mode ensemble.

Glosea4 ensemble members initialised on a particular start-date share exactly the same initial conditions and differ only due to the stochastic physics schemes used to represent model uncertainties.

Only four members from Glosea4 have the same lead time as the 51 members in the ECMWF ensemble. Some Glosea4 ensemble members are initialized 3 days before the ECMWF ensemble members.

The two start dates straddling the nominal start (Thursday) of the multi-model forecast are chosen so that Glosea fore- and hindcast share the lead time dependant systematic errors most closely.

Probabilities for each quintile category for the multi-model are defined as a simple weighted average of the 5 quintile probabilities (described in 2.4) from each individual ensemble. For each quintile the probability for the multi-model is:

Pmulti = (Pecmwf * 51 + Pglosea4 * 28) / (51 + 28)

The same weighting is applied to the multi-model hindcast although the hindcast sizes (70 and 84) are closer in the two models than the forecast ensemble sizes (51 and 28). (The weighting in favour of the larger ECMWF ensemble was made after comparing the skill scores for the single models. The intention is to give the multi model the best chance to succeed. Glosea4 scores for temperature and precipitation over Europe at extended lead times are lower than ECMWF scores. (Not shown))

2.4. Post processing

The first four full calendar weeks (i.e. Monday to Sunday) of each forecast ensemble member are time averaged into 3 forecast lead times: Period 1 (forecast week 1, days 5 to 11), Period 2 (forecast week 2, days 12 to 18) and Period 3 (forecast weeks 3 and 4, days 19 to 32) are averaged together from daily data as shown in Figure 1. Forecast lead time is counted from the first day of the burst mode initialised (reference) ECMWF forecast. Lead times in the Glosea4 ensemble member vary according to the lagged initialisation. The forecast ensemble is counted into quintile categories: well below normal, below normal, normal, above normal and well above normal, where the quintile boundaries are defined at each grid point so that they split the hindcast into 5 equal categories. Dividing the count by the ensemble size ascribes percentage probability for each category at each grid point.

3. Data for verification

Gridded global observation proxies based on reanalysis data are used to verify the forecast and the hindcast. The advantage of such “pseudo observations” is their global coverage and the equivalent representation (resolution in time and space) to resolved scales in the model data sets. Use of ERA40 data (Uppala et al. 2005) to validate the hindcasts is a legacy from the operational FORMOST monthly forecast system (Becker 2004). The real-time multi-model forecast is compared to daily ECMWF deterministic short range forecast with 12-36 hours lead time.

The use of 12 to 36 hours high resolution deterministic forecasts is not a good substitute for real observations for verification purposes but is applied here for convenience. (12 to 36 hour forecast data are also used in Re-analysis (Dee 2013) and in observation simulation experiments (Becker

1996). The high observational data density over Europe in particular suggests a high quality of short range forecasts when averaged over large grid box areas). However, the choice of ECMWF high resolution short range deterministic forecasts as verification data may bias the verification in favour of the ECMWF monthly forecast system.
Near surface temperature, precipitation, mean sea level pressure and geopotential at 500 hPa on a 1.875 * 1.25 regular latitude-longitude grid are stored from hindcasts, forecasts and pseudo observations.
The observed quintile boundaries for each forecast/hindcast are derived from rank ordering period mean samples of observations from the period 1989 to 1998 (same as used in the legacy FORMOST system). Ten years provide too small a sample to derive smooth quintiles. To estimate more robust observed quintile boundaries, the sample size is increased in the following way: for each year, the period mean is recalculated 21 times by shifting the period window along the time line. This increases the sample size to 210, 21 period means from each year. The rationale is that any 7-day period in a 21-day time window serves as a candidate member for such a pragmatic estimate. The 210 member sample describes inter annual variability of period averages for a particular calendar date. Climate change and decadal variability that may render the climatology of the 1990s different from the current climate are ignored. It is further assumed that the model hindcasts (1996 to 2009) sample the same climatology.

The Wheeler and Hendon (2004) real-time MJO index is used to derive composites of MJO activity. It is based on the first two Empirical Orthogonal Functions (EOFs) of the combined fields of near-equatorially-averaged 850 hPa zonal wind, 200 hPa zonal wind, and satellite- observed outgoing long wave radiation (OLR) data.
(from http://cawcr.gov.au/staff/mwheeler/maproom/RMM/RMM1RMM2.74toRealtime.txt on Mar. 11th 2013).

4. Results

This section presents the generic response to MJO forcing on Europe and the impact of the MJO on predictive skill for this region. In Section 4.1 we will show the modeled remote response to MJO forcing over Europe, the suggested mechanism causing the remote response and the generic MJO teleconnection pattern in the northern hemisphere, derived from a composite analysis of monthly hindcasts. Section 4.2 includes the impact of combining ECMWF with Glosea4 monthly forecasts and the impact of MJO activity on ROC scores derived from verification of one year of real-time monthly multi-model forecasts.

4.1 MJO composite analysis of the model hindcast data

A composite analysis based on observed MJO events is applied to the model hindcast data to investigate whether the multi-model system is able to reproduce the teleconnection seen in observational studies.

The monthly forecast lead time of up to 32 days provides a unique opportunity to investigate aspects of propagation of the MJO through the forecast system. Wheeler and Hendon's observation data describes the phase, amplitude and date when a particular MJO phase has been observed. To capture MJO phases likely to exert a teleconnection, only strong events (MJO index > 1.5) are selected. Collecting all hindcasts with a strong MJO phase near initialisation time forms the set of composite members for that particular MJO phase. The composites for each of the eight phases form a generic description of the MJO. This sampling exercise is repeated for the ECMWF hindcast, the Glosea4 hindcast and for observations. The hindcasts are initialised with a realistic description of the state of the atmosphere. Composites of strong MJO events in observations and hindcasts close to initialisation are expected to be very similar as model error has not yet had the chance to grow (Figure 2). Comparisons of hindcast means and observed composites at 10 and 20 days lead time may be used to investigate how closely the evolution of the MJO in the model hindcasts matches the observed evolution in MJO. As measure of the MJO we use precipitation and geopotential height at 500 hPa.

The composites are created as follows:

1. from the Wheeler and Hendon data set choose an MJO event date when the amplitude in one phase is larger than 1.5
2. Choose the closest initial date from the hindcast (each date corresponds to a Thursday, see above) pre-dating the event date chosen in 1, so that the MJO event occurs early in the hindcast. For Glosea4, hindcast members from dates straddling this hindcast date are chosen. See Fig.1
3. Average the first 7 day period of this hindcasts ensemble mean (this will include the observed MJO event).
4. Subtract the base-line monthly (day 1-32) mean hindcast climatology from the 7-day mean to create an MJO anomaly.
5. Repeat for each MJO event and average the anomalies from 4) by MJO phase.

Double counting an MJO event (although very rare) is accepted. This occurs when the MJO switches phase during the same week and for runs of consecutive days of high amplitude MJO. A 7-day mean is used to create composites rather than single days in accordance with the findings

by Cassou (2008) and others who ascribe a nominal persistence to each MJO phase of about 7 days and also because this is a typical period average used in monthly forecasts.

Observations and hindcast ensemble means from November to March over the period 1996 to 2009 are filtered for MJO activity as described above.
Each hindcast consist of 5 (ECMWF) to 6 (Glosea4) ensemble members. Averaging hindcast members filters out variability on the synoptic timescale. Composites of hindcast means for three lead times are formed for each of the eight phases of the MJO.

C	D	E
T+0: composite the first seven day mean anomaly of the MJO event from the hindcast initialized **closest** to the observed MJO event	**T+10:** composite the seven day mean anomaly **10 days after** the MJO event from the hindcast initialized closest to the observed MJO event	**T+20:** composite the seven day mean anomaly **20 days after** the MJO event from the hindcast initialized closest to the observed MJO event

Table 1: *MJO composites with 0, 10 and 20 days lag with respect to observed MJO events are compiled from ECMWF, Glosea4, multi-model hindcast and from ERA-40 observations.*

Composite C (T+0) provides a snapshot of teleconnections when an extreme phase of the MJO is present in the initial conditions and composites D (T+10) and E (T+20) describe how the MJO and corresponding teleconnections are sustained during the forecast period.
Composite C is derived from forecasts close to initialization time and should therefore resemble the composite of observed phases of the MJO very closely. To reduce the number of figures, MJO composites of phase 2 and 3, 4 and 5, 6 and 7, and 8 and 1 are pooled together as in Vitart and Molteni (2010).

Phase	2	3	4	5	6	7	8	1
Number	45	90	67	62	70	79	56	32
Composite size	135		129		149		88	

Table 2: *Number of MJO events during the extended (boreal) winter season, November to March during the hindcast period 1996 to 2009 for each phase of the MJO and composite size of 7-day averages.*

Figure 2 shows the evolution of the MJO along the equator in the component models compared with ERA-40. Weekly mean MJO phase composites for precipitation anomalies in composite C (see Table 1) show MJO activity captured close to start time of the model runs. Precipitation is

suppressed throughout the tropical belt apart from the land regions over India, the maritime continent and the western hemisphere (South America and Africa). The intensities of rainfall are the highest over the eastern Indian Ocean during MJO phase 2/3, the maritime continent during MJO phase 4/5, the Southern Pacific convergence zone during MJO phase 6/7, and the western hemisphere during MJO phase 8/1.

The multi-model components agree remarkably well with each other. The reanalysis precipitation anomaly pattern on the right matches the pattern of the model composites quite well over the eastern hemisphere. Over the western hemisphere however, the observed precipitation anomaly pattern indicates preferred rainfall over land (Southern America and Africa) rather than the tropical Atlantic Ocean. The reanalysis precipitation anomaly pattern over the western hemisphere varies hardly at all with the phase of the MJO. This may be an artifact of the sample size to describe synoptic variability. Anomalies are expressed as monthly means subtracted from single weekly means. The model composites are based on hindcast averages that appear much smoother than the reanalysis composites. Figure 2 confirms that the initial conditions of the multi-model components capture the MJO. To find signs of teleconnections with phases of the MJO we focus on model results, because the signal in the observation based composite is more difficult to identify due to the smaller sample size.

Figure 3 shows the remote response to MJO forcing over Europe. Composite D (T+10) is plotted for the northern hemisphere Z500 anomalies. The composite shows 7-day average hindcast anomalies from the hindcast monthly mean climatology for ECMWF (left) and Glosea4 (middle). Ten days into the forecast with an MJO phase 2/3 identified in the initial conditions, south Western Europe and the north Pacific are dominated by high geopotential while Eurasia is showing reduced geopotential. This pattern resembles a positive NAO phase. In response to MJO phase 4/5 in the initial conditions the overall pattern is slightly reduced in amplitude and appears rotated eastward by about 30 degrees, resembling a positive NAO phase but weaker and shifted. Ten days after MJO phase 6/7 the Z500 anomaly pattern over Europe changes sign showing higher geopotential near Iceland and lower over western and central Europe. This pattern is similar to a negative NAO phase. The model composites appear to agree better with each other than with the reanalysis as they appear smoother due to ensemble averaging. The core pattern however, changing sign of the NAO in response to the MJO can be seen in the observations as well as in the multi- model components, in particular in response to MJO phases 2/3 and 6/7.

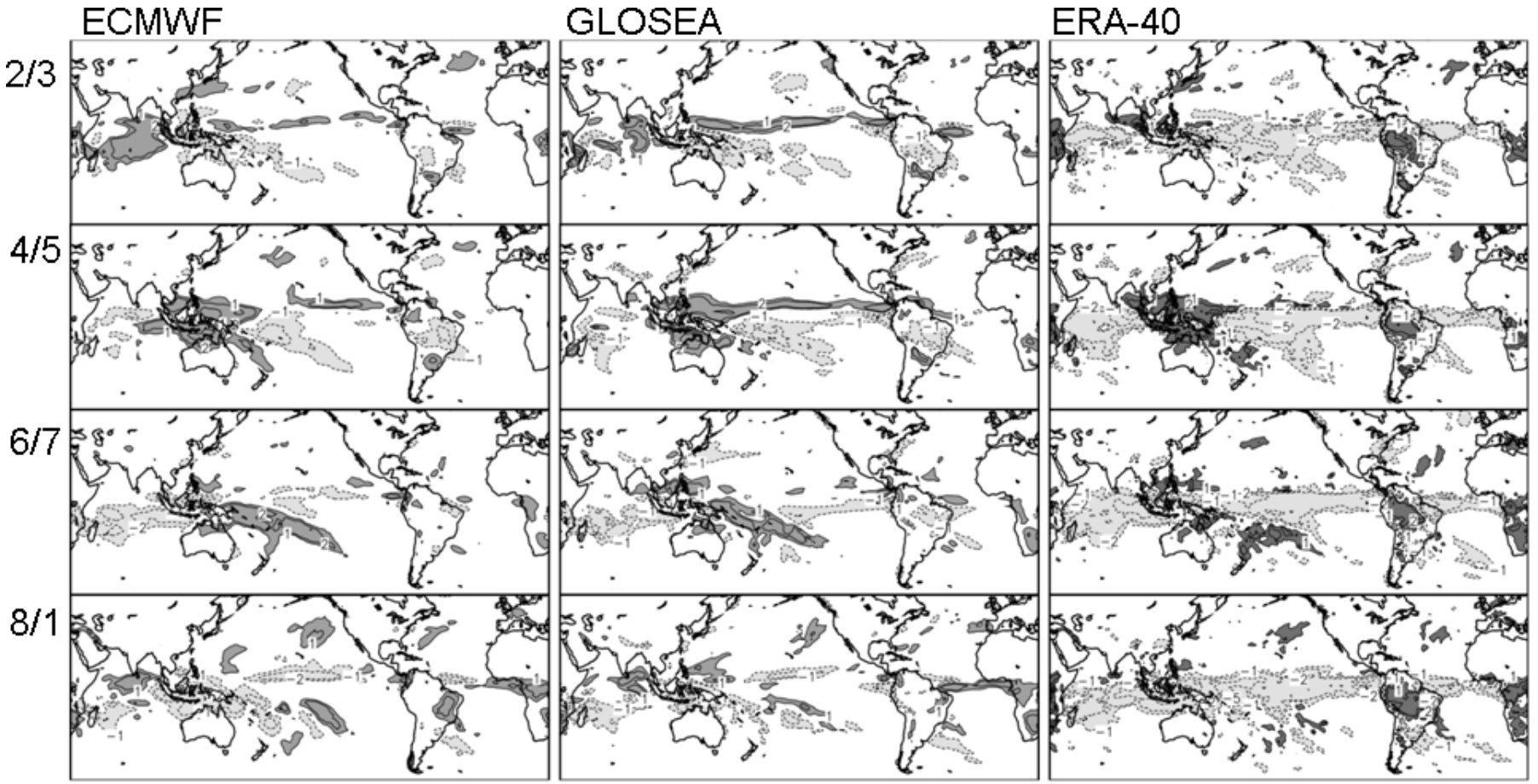
ECMWF
GLOSEA
ERA-40
2/3
4/5
6/7
8/1

Figure 2: *Weekly mean MJO phase composites for precipitation anomalies close to initial forecast time (Composite C). ECMWF left, Glosea in the middle and ERA-40 right. The composites show weekly mean precipitation anomalies when MJO in phase 2 and 3, 4 and 5, 6 and 7 and 8 and 1 with an amplitude > 1.5 is present for at least one day during the first week of the hindcast. Positive anomalies are shaded dark, negative anomalies are shaded light grey. Contours +/-1, 2 and 5 mm/d are plotted.*

Confirming the observed relationship between MJO and NAO reported by Lin and Brunet (2009), over Europe the response to MJO 2/3 is a switch towards a positive NAO and after MJO phase 6/7 the NAO appears in its negative phase. Both component models in the multi-model confirm that the NAO tends to reverse sign in response to the MJO. These MJO phases are also more common than phases 4/5 and 8/1 (see Table 2). However, the modeled response pattern appear more similar with each other than with the observed response patterns because the ensemble averaging introduces a degree of smoothing of synoptic activity that is absent from the re-analysis based composite. Synoptic variability on this timescale is high in particular over the mid latitudes and Europe. Due to the ensemble averaging the amplitude of the MJO induced signals in the models is somewhat smaller than observed. The hindcasts consist of 5 to 6 parallel realizations that average out synoptic noise which is retained in the observed composites. The sample size in the observed composites on the other hand is 5 to 6 times smaller than in the hindcast mean composites. Therefore, the focus is switched to model results for a more robust assessment of the modeled influence of the MJO on predictive skill in monthly forecasts over Europe.

To illustrate drivers of the remote response to MJO forcing multi-model hindcast average anomalies are shown in Figure 4 for MJO phases 2/3 and in Figure 5 for MJO phases 6/7. The column on the left (composite C (T+0)) shows the MJO phase captured near initialization time of the hindcast runs. Both model hindcasts are initialized with reanalysis data. Therefore, composite C resembles observations more closely. The column on the right (composite D (T+10)) shows how the MJO evolves with increasing forecast lead time. The pathways for action from the MJO into the European mid latitudes may be described as follows: Enhanced convection in the west Pacific warm pool/maritime continent 10 days after MJO phase 2/3 is captured in the initial conditions (Figure 4 d) emits a Rossby wave response along the Pacific-North-America (PNA) pattern linking with a positive North Atlantic Oscillation (NAO+) (Figure 4 b).

Composite D, 10 days after an MJO event in phase 2/3 is captured in the initial conditions (Figure 4 d), clearly shows positive precipitation anomalies in the central Pacific, indicating enhanced convection which acts as a source of gravity wave activity, emitting a Rossby wave train impacting on the PNA/NAO pattern (Figure 4 b). The anomaly pattern over Europe resembles a positive NAO phase. Deep convection and heat transfer to the troposphere is enhanced during MJO events. This tropical forcing generates atmospheric Rossby waves that propagate pole ward and eastward and are subsequently refracted back to the tropics.

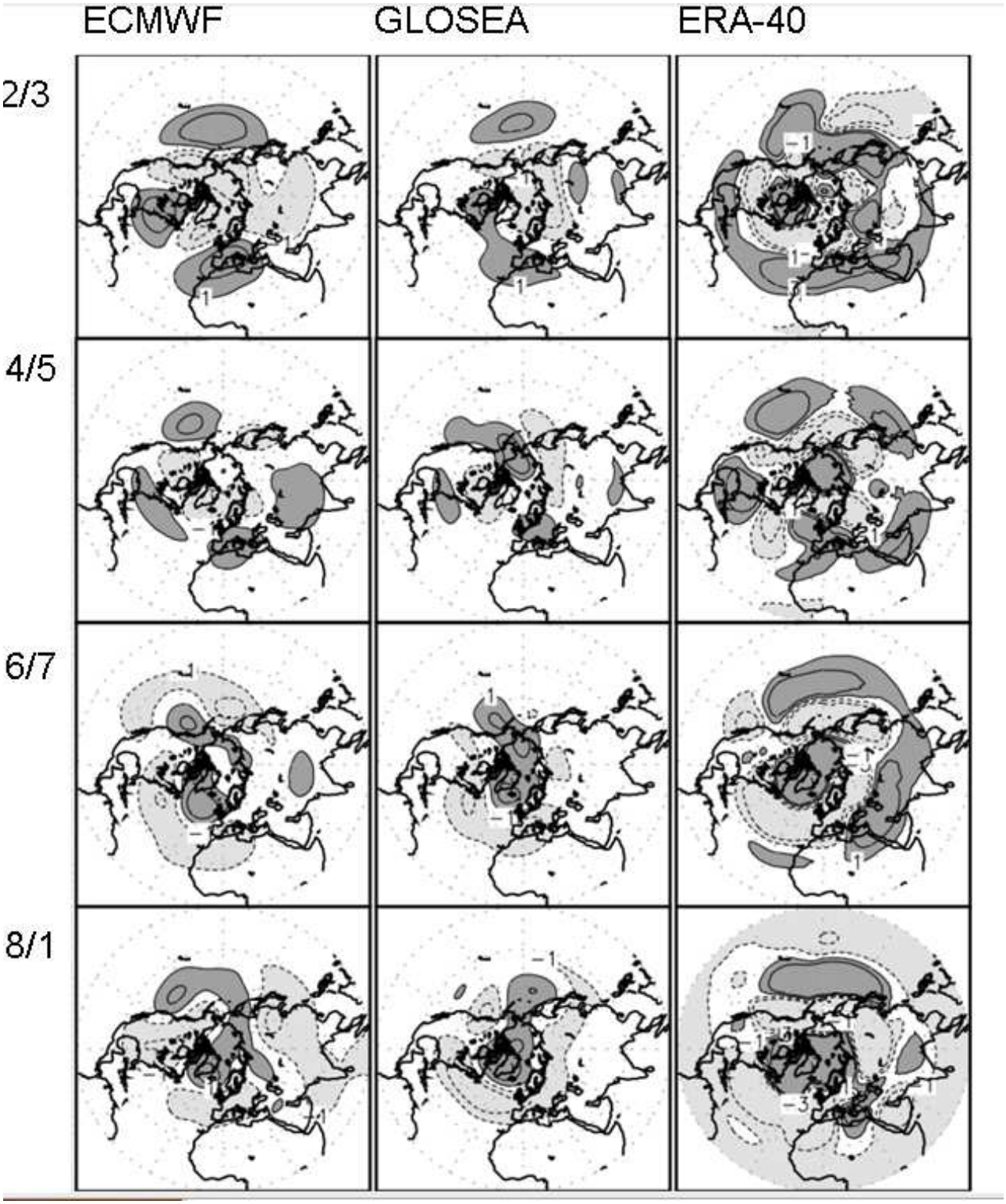

Figure 3: *Composites of Z500 anomalies 10 days after an MJO event has been identified in the initial conditions (composite D). ECMWF is shown on the left, Glosea in the middle and ERA-40 right. The composites show weekly mean Z500 anomalies 10 days after an MJO in phase 2 and 3, 4 and 5, 6 and 7 and 8 and 1 was present near the initialization of the hindcast. Positive anomalies are shaded dark, negative anomalies are shaded light grey. Contours +/-10 and 30 m are plotted.*

Poleward propagating Rossby waves explain many of the observed statistical teleconnections between low latitude and high latitude climate, as shown in the study by Hoskins and Karoly (1981).

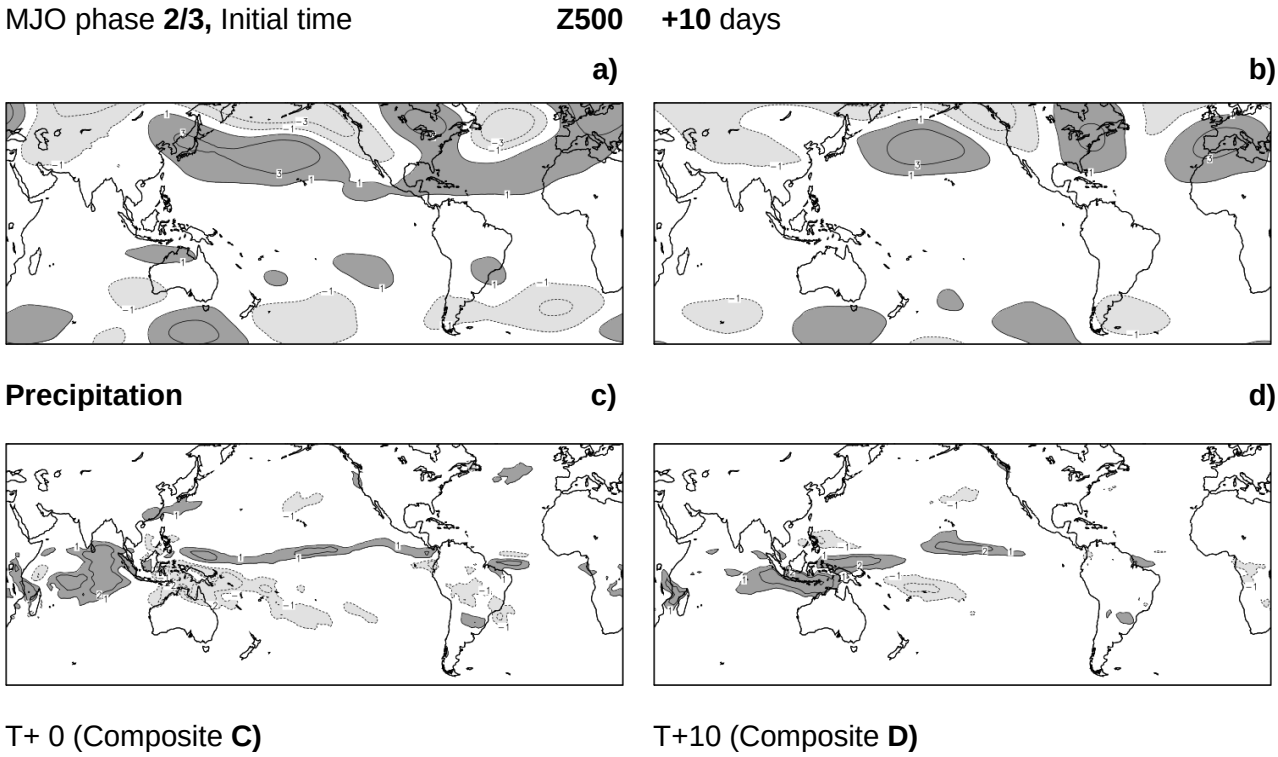

Figure 4: *The Multi–model lagged composite phase 2/3 of the MJO. The column on the left (composite C) shows the MJO phase 2/3 captured near initialization time of the hindcast runs. Composite D (10-days into the forecast) is shown on the right. Z500 anomalies are shown in the top 2 panels (panels a, b) and Precipitation is shown in the bottom 2 panels (c, d). Positive anomalies are shaded dark, negative anomalies are shaded light grey. Contours indicate +/-1, 2 and 5 mm/d and +/-10 and 30 m.*

Poleward propagating Rossby waves are an important and unambiguous part of the variability in the Northern Hemisphere, as expressed in the Pacific North America pattern. Composite D for Z500 10 days after an MJO event in phase 6/7 (Figure 5 b) shows a clear Rossby wave train emitting from the tropical West Atlantic reversing the NAO pattern. Ten days after MJO phase 6/7 the Z500 anomaly pattern over Europe changes sign showing higher geopotential near Iceland and lower geopotential over western and central Europe resembling a negative NAO response (Figure 5 b). Confirming the findings of recent modelling studies by Cassou (2008) and Vitart and Molteni (2010), the NAO tends to reverse sign on the monthly forecast time range if a strong MJO is captured in the initial conditions.

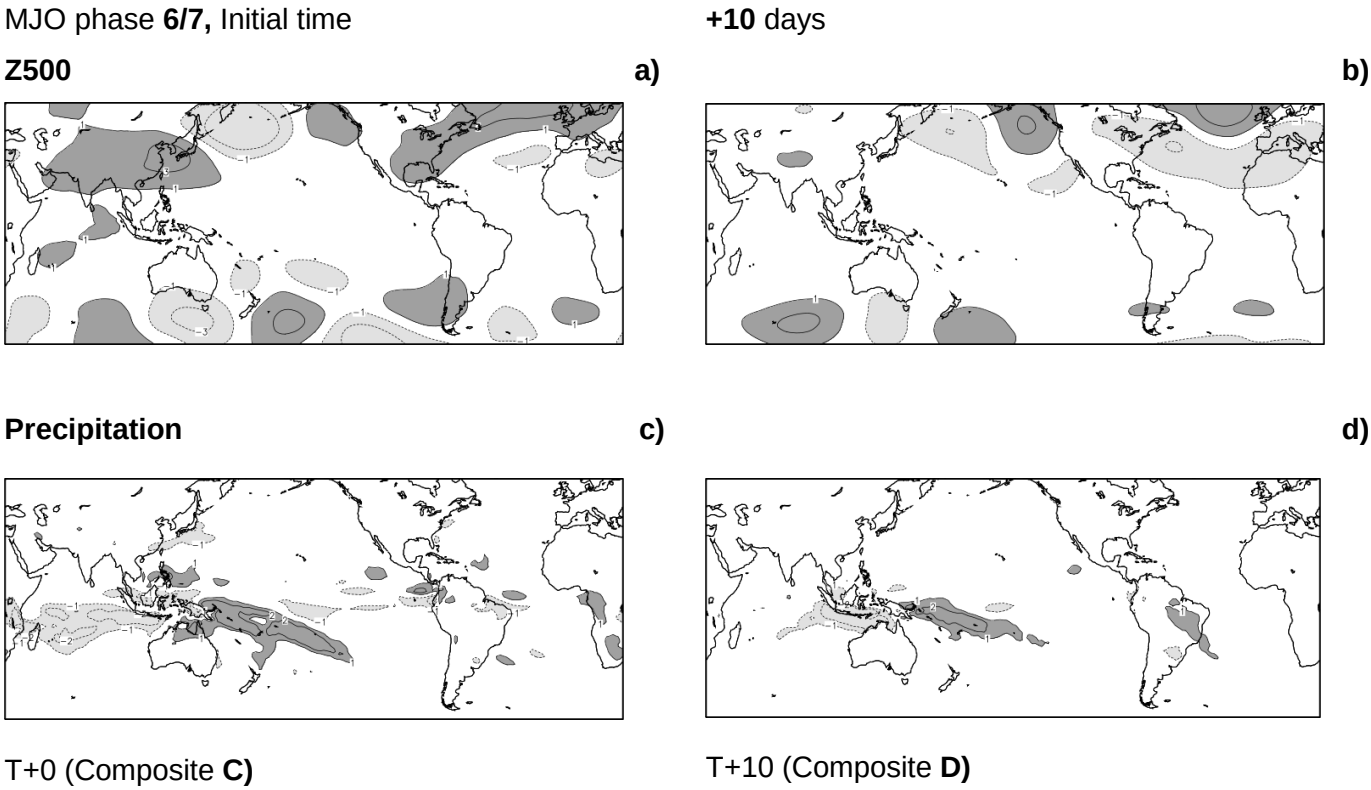

Figure 5: *The multi–model lagged composite phase 6/7 of the MJO. The column on the left shows the MJO phase 6/7 captured near initialization time of the hindcast runs (composite C). Composite D (10-days into the forecast) is shown on the right. Z500 anomalies are shown in the top 2 panels (a, b) and precipitation is shown in the bottom 2 panels (c, d). Positive anomalies are shaded dark, negative anomalies are shaded light grey. Contours indicate +/-1, 2 and 5 mm/d and +/-10 and 30 m.*

The large set of hindcasts from the two state-of-the-art monthly forecast models suggests a generic mechanism by which the MJO influences predictability on the sub-seasonal time scale.

To gauge the total signal of MJO forcing on the northern hemisphere the difference between the response pattern to MJO forcing in phase 6/7 and 2/3 is calculated. Figure 6 shows the generic MJO teleconnection patterns in Z500 at the start of the forecast and at 10 and 20 days forecast lead time. The response to MJO is mainly driven by changes in tropical precipitation and the associated large scale response to gravity waves induced by deep convective heating anomalies (Moore et al. 2010, Allen et al. 2008).

Significance of the generic MJO composite pattern is assessed by bootstrap re-sampling (with replacement). From the complete hindcast archive constituting 350 hindcast mean anomalies (25 initialization times during November to March from 14 year hindcasts) two random samples of 135 and 149 members matching the composite sizes of MJO phase 2/3 and MJO phase 6/7 (see Table 2) are selected. The difference between the random samples is calculated. This selection is repeated 1000 times. The set of 1000 random sample differences is rank ordered and the 1st and the 99th percentile are chosen as significance thresholds. Where the MJO composite pattern

exceeds either threshold there is evidence that the signal in the composite exceeds the underlying noise at the 1% level.

The left column in Figure 6 shows the generic MJO response in Z500. To maximize the amplitude of the response signal to MJO forcing the difference between MJO composites is shown from phases 6/7 minus phases 2/3. Near initial time of the hindcasts (top) a clear PNA pattern can be seen. The associated precipitation anomaly (Figure 7) shows active convection in the north western tropical Pacific, near the Philippines and over the South China Sea. By 10 days later the Z500 anomalies on the European sector have grown and show a clear negative NAO pattern. The associated tropical precipitation anomaly diminishes where it was most active ten days earlier. Twenty days into the forecast, the precipitation anomalies in the west Pacific have all but vanished and new centres of convective activity emerge nearer the western hemispheric warm pool (wider seas around Central America) and over the tropical Atlantic. These precipitation anomalies show an associated short arched Rossby-wave response into Europe in the Z500 field and appear to sustain the influence of the MJO on the NAO (Hoskins et al. 2012). Occasionally, such tropical – extra tropical connections are associated with extreme weather events in mid-latitudes that are linked to atmospheric rivers and may cause flooding (Guan et al. 2012, Lavers et al. 2011).

The composite analysis of the MJO in the multi-model hindcast suggests a possible mechanism that promises improved skill in predictions over Europe on the sub-seasonal time scale. But does the MJO teleconnection actually improve skill scores in real-time forecasts?

4.2. Verification of the real-time forecast set

Forecast quality is a multidimensional concept described by several scalar attributes that provides useful information about the performance of a forecasting system. No single measure is sufficient for judging and comparing forecast quality. However, for brevity, forecast quality is evaluated using only the area under the ROC curve. The ROC skill measure is described in Thornes and Stephenson (2001), Jolliffe and Stephenson (2003), Doblas-Reyes et al. (2003) and Mason (2004).

The three sources of uncertainty in common scoring metrics of probabilistic forecasts: insufficient number of forecast cases, improper estimates of probabilities from small-sized ensembles and imperfect reference values due to observation errors, are addressed in the following way: We use the ROC score to assess 55 full size ensemble forecasts with respect to realistically initialized short-range weather forecasts on the monthly forecast grid resolution over Europe (13W - 30E, 35N - 65N, 600 grid points). The ROC score is calculated for the outer quintiles for period averages of temperature and precipitation during the period May 2011 - May 2012.

Generic MJO teleconnection pattern: MJO phases 6/7 minus phases 2/3 in **Z500**

Model: Observed:

Composite **D**

T+0

Early

Composite **C**

T+10

+10 days

Composite **E**

T+20

+20 days

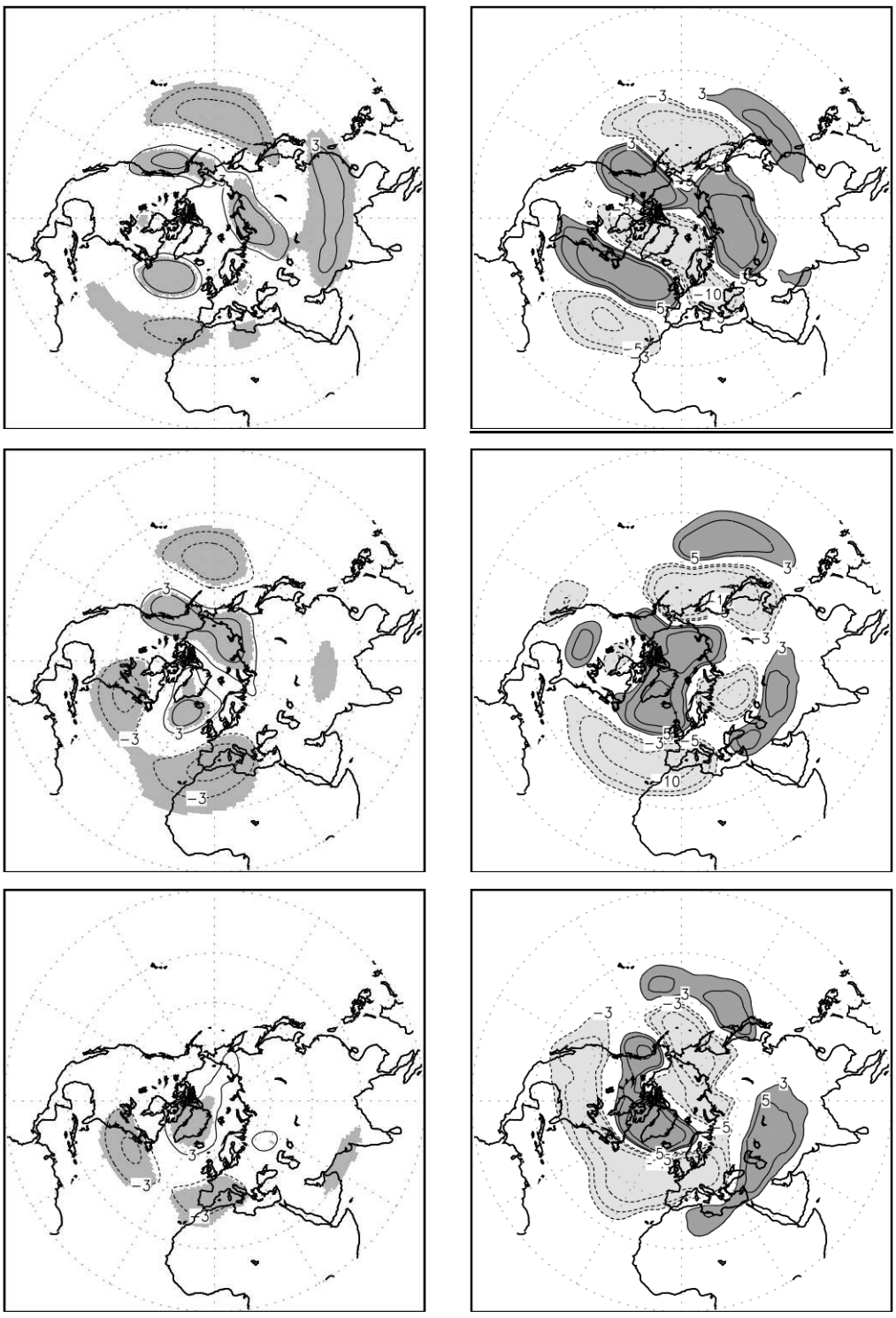

Figure 6: *The generic MJO teleconnection in Z500 on the northern hemisphere. Composite C (near initial time) is shown on top, 10 days lead (D) is shown below and 20 days (E) lead is shown at the bottom. The light grey shading (left) indicates significance at the 1% level. Images on the right show the MJO teleconnection in observed Z500. The 3 panels on the right show observed Z500 anomalies. Positive anomalies are shaded dark, negative anomalies are shaded light grey. Contours indicate +/-10 and 30 m.*

Generic MJO teleconnection pattern: MJO phases 6/7 minus phases 2/3 in **Precipitation**

Model: Observed:

Composite **D**

T+0

Early

Composite **C**

T+10

+10 days

Composite **E**

T+20

+20 days

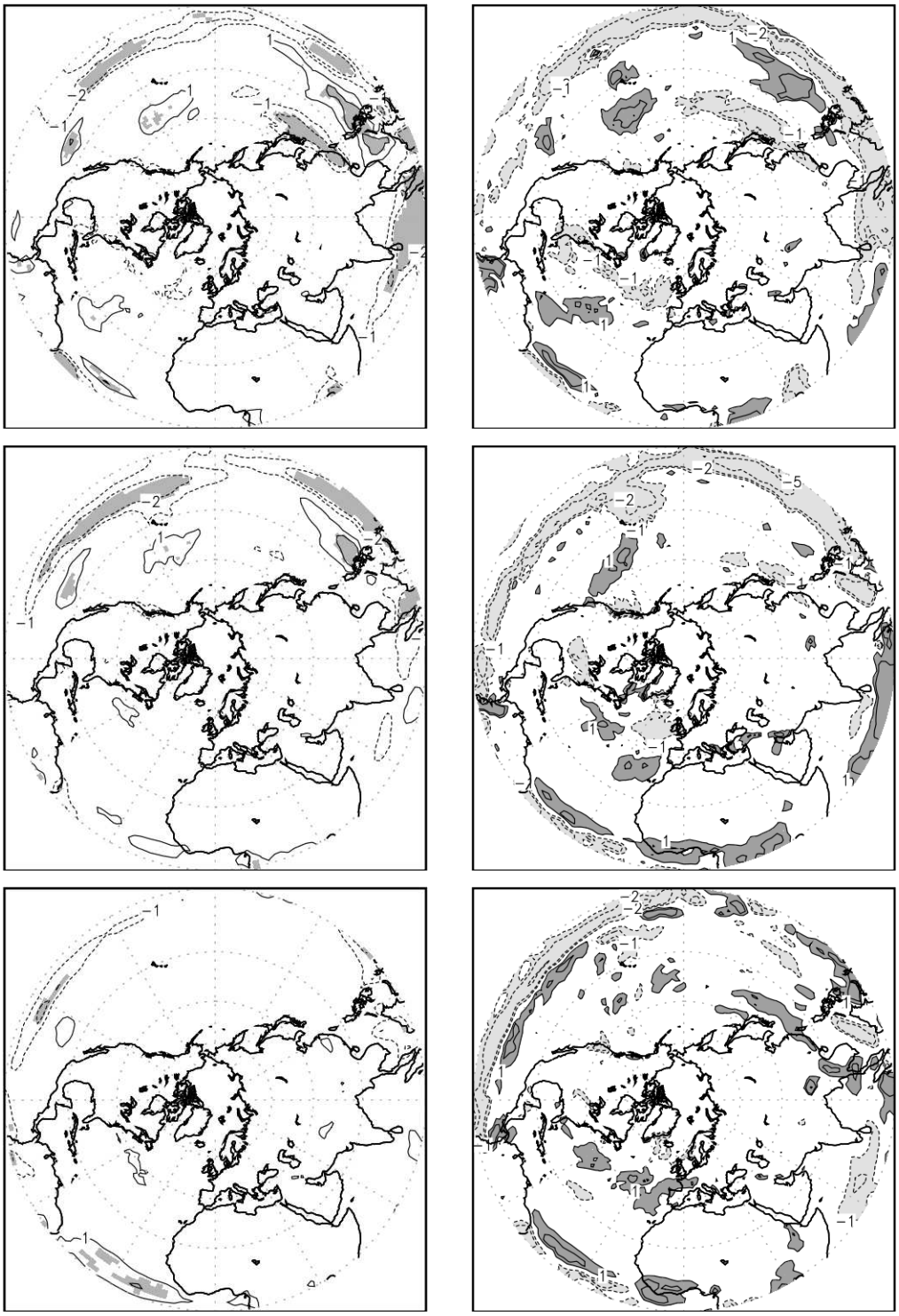

Figure 7: *The generic MJO teleconnection in precipitation on the northern hemisphere. To maximize the amplitude of the response signal to MJO forcing the difference between MJO composites is shown from phases 6/7 minus phases and 2/3. Composite C (near initial time) is shown on top, 10 days lead (D) is shown below and 20 days lead (E) is shown at the bottom. The light grey shading (left) indicates significance at the 1% level. Images on the right show the MJO teleconnection in observed precipitation. Positive*

anomalies are shaded dark, negative anomalies are shaded light grey. Contours indicate +/-1, 2 and 5 mm/d.

Real-time forecasts unlike most hindcasts have the full ensemble size and therefore the skill assessment offers more reliable results. The ensemble size in forecasts (51 and 28) is much larger than in individual hindcast years (5 and 6). The greater ensemble size yields a more robust estimate of outer quintile probabilities than is possible to derive from the individual small ensemble hindcast simulations. Therefore, full ensemble size real time forecasts offer a better basis to estimate probabilistic skill.

The outer quintile categories on average achieve higher scores than the quintiles closer to the climatological mean. Outer quintiles are also more important for predicting moderately extreme weather anomalies. Skill scores for moderately cold temperatures (Quintile 1) and low precipitation on lead times beyond the medium range (week 2 and week 3&4) are shown. The verification study investigates two questions:

- does the multi-model show better skill than the ECMWF model alone and
- does the MJO present "windows of opportunity" for better monthly forecasts over Europe?

The impact of the multi-model on real-time forecast skill is assessed by verifying the complete set of real-time forecasts from ECMWF and from the multi-model. The impact of the MJO on real-time forecast skill is demonstrated by verifying the subset of 30 real-time forecasts considering "windows of opportunities" that may arise from strong MJO anomalies during the initialisation.

Investigating two sets of forecasts for two variables (T and P) and for two lead times (Period 2, days 12 to 18) and Period 3 days 19 to 32) provides 8 comparisons in total. ROC scores for the lower quintiles of well below normal temperature and well below normal rainfall are presented in Table 3.

The ECMWF and the multi-model show skill (ROC > 0.5) for temperature and precipitation forecasts over Europe for lead times 12 to 18 days. For lead times into the second half of the month (Period 3), however, ROC scores are smaller. The multi-model scores marginally higher than the ECMWF model for temperature in Period 2 and for precipitation in Period 3. Precipitation forecasts in Period 2 with the ECMWF model are as skilful as the multi-model.

The impact of the MJO on forecast skill is small. Scores for temperature forecasts are slightly lower during forecast Period 2 but higher in the single and in the multi-model in Period 3. Precipitation forecasts with MJO activity during initialization however score marginally higher on both lead times.

For Europe, winter (December, January and February) forecasts are generally more skilful than other seasons. A further stratification of the forecast sample by season, however, did not add to the results presented above. Mainly because 11 out of 14 forecasts during winter had some MJO activity during initialization, the forecast sample is much smaller (14 rather than 55) and the results were very similar.

We use the method by Hanley and McNeil (1982) to determine how large sample sizes should be to ensure that one can statistically detect differences in the performance of forecasting systems. Assuming the 600 grid points over Europe in the verified fields were independent in space and time, ROC score differences of 0.01 appear to be significantly different at the 5% level. However, grid fields present a large redundancy of independent information. The true number of degrees of freedom in a grid field of temperature and precipitation may be compared with the number of empirically classified weather types (Fraedrich et al. 1995). Over Europe this is nearer to 29, assuming that "Grosswetterlagen" (James 2007) describe European weather patterns succinctly. For a reduced number of degrees of freedom of 29, commensurate with the number of independent European weather types (synoptic large scale weather patterns) the required difference in the skill scores to be statistically significant rises to over 0.1.

	Period 2		Period 3	
	Temperature			
	ECMWF	Multi	ECWMF	Multi
All year (1)	.72	.73	.63	.60
MJO(2)	.69	.71	.64	.61

	Period 2		Period 3	
	Precipitation			
	ECMWF	Multi	ECMWF	Multi
All year(1)	.68	.68	.55	.56
MJO(2)	.70	.70	.58	.57

Table 3: Lower quintile ROC scores for temperature and precipitation over Europe. Period 2 describes week 2 and period 3, week 3 and 4. ROC scores over 55 forecasts and over 30 forecasts with MJO activity in the initial conditions are shown. Orange indicates higher skill scores over Europe when MJO activity is captured in the initial conditions. Blue indicates where the ECMWF scores higher than the multi-model. Grey indicates higher ROC score without MJO forcing. However, differences in ROC scores due to the multi-model combination or the MJO in the initial conditions are not statistically significant.

The largest difference in skill scores in our assessment is just 0.03 in two out of eight test cases. Hence, we conclude that the presented skill scores are not statistically different.
The results section may be further summarized in that:

- A generic teleconnection of the MJO with the NAO is operative in both components of the multi-model, albeit weaker than observed.
- The multi-model shows similar skill to the single ECMWF model.
- MJO activity in the initial conditions of the ensemble makes no significant difference in skill on sub-seasonal lead times in this model setup.
- Differences in ROC scores are small and not statistically significant.

5. Discussion

A multi-model ensemble prediction system for the monthly (sub-seasonal) time range was investigated for improvement over its single model predecessor and for conditional skill improvement due to the MJO. The combination of the operational monthly forecast system from ECMWF with the Glosea4 system at the Met Office in a multi-model forecast system as described above shows no statistically significant improvement over using a single model. The initially appealing choice of ECMWF high resolution short range deterministic forecasts as verification data may bias the model comparison in favour of the ECMWF monthly forecast system. Marginally better skill scores related to the impact of MJO activity in the initialization are not statistically significant. The response to tropical anomalous heating due to convection associated with the MJO appears to be a promising candidate for better monthly forecasts for Europe, if the MJO teleconnection patterns were better resolved in the multi-model.
The skill improvement due to the ECMWF – Glosea4 multi-model combination is small and not statistically significant. Further skill improvement was expected to be achieved in forecast situations with strong MJO activity in the initial conditions of the predictions. Such forecasts show no statistically significant higher skill in the monthly forecast setup described here.
A composite study of the model hindcasts confirmed the observed teleconnection of the MJO with weather over Europe. Enhanced convection in the vicinity of the western hemisphere warm pool may force a wave response impacting on Europe more efficiently in the multi-model than in each individual model and therefore may increase skill for monthly prediction in Europe. This composite analysis based on observed MJO activity differs from the way the MJO has been examined by Vitart and Molteni (2010) who recalculate the MJO index from the ECMWF model fields of OLR, and u-wind components at 850 and 200 hPa and then further sub select by the speed of the MJO. Vitart and Molteni (2010) average forecast periods over 15 days to describe the response to MJO forcing rather than 7 days in this study. Cassou (2008) describes response to the MJO over

Europe from counting individual days. Differences in period averages describing MJO phases between this study and the studies of Cassou (2008) and Vitart (2010) make a direct comparison of MJO teleconnections with Europe as described here more difficult. We observe no statistically significant improvements to sub-seasonal forecasts for Europe due to MJO activity in the initial conditions of full ensemble forecasts. The lack of skill improvement for predictions over Europe on the monthly timescale may be explained by the subtle differences between the model responses to phases of the MJO (and associated different tropical heating anomalies, not shown). Figures 4 and 5 show only small anomalies associated with MJO teleconnections. This could be an artefact of the hindcast ensemble averaging, where some of the chaotic, synoptic weather variability is removed but more likely confirms the genuine lack of an MJO signal over Europe in this multi-model forecasts setup. MJO biases in model climates can be related to how effectively the moisture-convection relationship is represented in the model and most of the current generation of general circulation models have serious deficiencies in representing this relationship (Xavier, 2010). Some of the low amplitude MJO teleconnection patterns shown above may result from the rate at which the model drifts from its initialised moisture-convection relationship towards its own characteristic state (Shelly 2013). The air-sea coupled system involves complex interactions that could amplify the rate of initial error growth (Klingaman 2013). These results highlight the potential importance of coupled initialisation that simultaneously minimises cost functions for atmosphere and ocean. Detailed diagnostics of the model diabatic heating in short range forecasts and in long term climate simulations may improve our understanding of the initial error development.

These results further indicate that it may be possible to improve skill in sub-seasonal forecasts in the northern extra tropics with an improved tropical initialization, a better prediction of the tropical MJO and a better representation of the tropical-extra tropical interaction in dynamical models.

Precipitation forecasts initialized with MJO activity however are statistically as skilful as the skill scores compiled from the complete forecast archive suggest. The multi-model shows statistically equal skill as the ECMWF model. The small differences between ROC scores are not statistically significant and we conclude that neither the multi-model nor the MJO as described above does improve monthly forecast skill in this multi-model setup. The choice of other descriptions of reality than the ECMWF high resolution short range deterministic forecasts as verification data might show the model comparison more in favour of the multi model. An analysis of the degree of realism described by observation based verification data sets is beyond the scope of this study.

The combination of the forecast members from a lagged and a burst mode initialized ensemble needs to be carefully considered. Thursday highlights the start and centre day of the burst and lagged ensemble. Matching the lag mode initialized Glosea4 ensemble members with the burst mode initialized ECMWF ensemble as described in Figure 1 means that only four members from Glosea4 have the same lead time as the 51 members in the ECMWF ensemble. Some Glosea4

ensemble members are initialized 4 days before the ECMWF ensemble members. Comparing the two multi-model components in this way, the lagged initialised ensemble is disadvantaged compared with a burst mode initialized ensemble.

Operational monthly range forecasts may be made on the basis of combining prior knowledge with the raw forecast from multi-models. This procedure is gaining momentum in seasonal predictions. Prior knowledge of climate variability, the current state of the climate system and known model deficiencies are taken into account every time a new forecast is issued. The interpretation of multi-model forecasts may be guided by the realism of simulated teleconnections present in the hindcast. Observed large scale anomaly patterns at initial time of the forecast add preliminary information about the confidence in the current forecast. Models with errors in teleconnection patterns relevant to the current forecast situation may be ignored from the multi-model. Paying attention to the current state of slow components of the climate system and their teleconnections may lead to a better understanding of climate variability and its impact on predictability for Europe on the monthly time scale. Understanding the relation between predicted anomalies and their forcing mechanisms may greatly improve confidence in monthly predictions in particular of moderately extreme events (outer quintiles). It is therefore suggested to extend current offerings of monthly forecast products by descriptions of:

1. The current state of the slow components of the climate system including the MJO.
2. Teleconnection patterns during the forecast period.
3. A synthesis of currently predicted extreme events in relation to slow components and their teleconnections.

6. Future work

Upgrading the Met Office monthly prediction system to use the latest version of the Glosea system may offer scope for improved predictive skill. Realistically modelled teleconnections due to MJO activity in the initial conditions is a particular source of optimism. The analysis of MJO related teleconnections may be extended to other slow components of the climate system including coherent circulation pattern with lifecycles on sub-seasonal time scales. Organized tropical convection in its active phase results in a planetary wave response that modulates teleconnection patterns that influence the European region throughout the seasonal cycle and winter in particular. Organized tropical convection associated with the MJO is also strongly modulated by extra-tropical waves, including those that previously originated within the MJO itself. Such associations suggest the possibility that coupling between the tropics and the extra-tropics might be fundamental to the evolution and structure of the MJO. Associated global teleconnections modulate extreme weather

events. Since the multi-model tends to show no skill improvement due to the MJO, MJO modulation of extreme events would reduce our ability to predict such events at extended range until simulation of the MJO improves (P. Roundy 2011).

As rightly identified by Cassou (2008), however, the promised predictive skill improvement will not be fully realized until today's forecast models properly simulate not only tropical MJO dynamics but also the tropical-extra-tropical interactions that are integral to the evolution of the atmosphere on the global scale (Moore 2010). It is suggested to:

- Repeat the analysis on the Glosea 5 forecast system.
- Routinely consider the state of the MJO in the initial conditions to gauge confidence in extreme forecasts for Europe and the UK in particular.

Through the multitude of interactions of the MJO and various weather, climate and environmental components of the Earth system, better MJO predictions will provide valuable information for hazard response, resource managers and other decision makers.

Acknowledgements:

We thank Dr. Matthew Wheeler of the Centre for Australian Weather and Climate Research at the Bureau of Meteorology for making the MJO index available and Prf. Adam Scaife and Dr. Anca Brookshaw for useful discussions and encouragement. We are grateful two anonymous reviewers whose comments proved invaluable in improving the presentation of the material. This work was supported by the Joint DECC/Defra Met Office Hadley Centre Climate Programme (GA01101).

References:

Allen, G., G. Vaughan, D. Brunner, P. T. May, W. Heyes, P. Minnis, and J. K. Ayers (2008) Modulation of tropical convection by breaking Rossby waves. Quart. J. Roy. Meteorol. Soc., 135(638), 125–137, doi: 10.1002/qj.349.

Anderson, D., Sub-seasonal to seasonal prediction research implementation plan, WMO http://www.wmo.int/pages/prog/arep/wwrp/new/S2S_project_main_page.html (2013.03.15)

Arribas A, Glover M, Maidens A, Peterson K, Gordon M, MacLachlan C, Graham R, Fereday D, Camp J, Scaife AA, Xavier P, McLean P, Colman A, Cusack S, 2011: The GloSea4 Ensemble Prediction System for Seasonal Forecasting. Mon. Wea. Rev., 139, 1891–1910. doi: http://dx.doi.org/10.1175/2010MWR3615.1

Balmaseda, Magdalena A., Arthur Vidard, David L. T. Anderson, 2008: The ECMWF Ocean Analysis System: ORA-S3. Mon. Wea. Rev., 136, 3018–3034. doi: http://dx.doi.org/10.1175/2008MWR2433.1

Bernd Becker 2004: Development of Operational Forecasts for Monthly and Seasonal Timescales (FORMOST). STAGE PLAN FOR FORMOST2. http://www-nwp/~frtm/formost/doku/Formost2_Stage_Plan_1.1.doc (on June 12th 2013)

Bernd Dieter Becker, Hervé Roquet, Ad Stoffelen, 1996:
A simulated observation data base including ATOVS, ASCAT and DWL data, Bulletin of the American Meteorological Society. Vol. 77, No. 10, October 1996

Blackburn, M., D. L. Williamson, K. Nakajima, W. Ohfuchi, Y. O. Takahashi, Y.-Y. Hayashi, H.,Nakamura, M. Ishiwatari, J. L. McGregor, H. Borth, V. Wirth, H. Frank, P. Bechtold, N. P. Wedi, H. Tomita, M. Satoh, M. Zhao, I. M. Held, M. J. Suarez, M.-I. Lee, M. Watanabe, M. Kimoto, Y. Liu, Z. Wang, A. Molod, K. Rajendran, A. Kitoh and R. Stratton, 2013: The Aqua-Planet Experiment (APE): CONTROL SST simulation. J. Meteor. Soc. Japan, 91A, this issue, doi:10.2151/jmsj.2013-A02.
Bougeault, P., Z. Toth, C. Bishop, B. Brown, D. Burridge, D. Chen, E. Ebert, M. Fuentes, T. Hamill, K. Mylne, J. Nicolau, T. Paccagnella, Y.-Y. Park, D. Parsons, B. Raoult, D. Schuster, P. Silva Dias, R. Swinbank, Y. Takeuchi, W. Tennant, L. Wilson and S. Worley, 2010: The THORPEX Interactive Grand Global Ensemble (TIGGE). Bull. Amer. Met. Soc., 91, 1059–1072.

Buizza, R., T. N. Palmer, 1995: The Singular-Vector Structure of the Atmospheric Global Circulation. J. Atmos. Sci., 52, 1434–1456.
doi: http://dx.doi.org/10.1175/1520-0469(1995)052<1434:TSVSOT>2.0.CO;2

Buizza, R., 1997: The singular vector approach to the analysis of perturbation growth in the atmosphere. Thesis submitted for the degree of Doctor of Philosophy (PhD) of the University of London, March 1997; available from the Department of Mathematics, U.C.L., Gower Street, London WC1E-6BT, UK.

Cassou., C., 2008, Intraseasonal interaction between the Madden–Julian Oscillation and the North Atlantic Oscillation Nature, Vol 455/25, doi:10.1038/nature07286

Dee, Dick, Fasullo, John, Shea, Dennis, Walsh, John & National Center for Atmospheric Research Staff (Eds). Last modified 14 Mar 2013. "The Climate Data Guide: Atmospheric Reanalysis:

Overview & Comparison Tables." Retrieved from https://climatedataguide.ucar.edu/reanalysis/atmospheric-reanalysis-overview-comparison-tables.

Doblas-Reyes, F.J., V. Pavan, and D.B. Stephenson (2003). Multi-model seasonal hindcasts of the NAO. Climate Dynamics, 21, 501-514, 10.1007/s00382-003-0350-4.

Fraedrich, Klaus, Christine Ziehmann, Frank Sielmann, 1995: Estimates of Spatial Degrees of Freedom. J. Climate, 8, 361–369.
doi: http://dx.doi.org/10.1175/1520-0442(1995)008<0361:EOSDOF>2.0.CO;2

Frederiksen, Jorgen S., 2002: Genesis of Intraseasonal Oscillations and Equatorial Waves. J. Atmos. Sci., 59, 2761–2781.
doi: http://dx.doi.org/10.1175/1520-0469(2002)059<2761:GOIOAE>2.0.CO;2

Jorgen Frederiksen (CSIRO Marine and Atmospheric Research, Aspendale, Australia) will speak on: "Tropical-Extratropical interactions of intraseasonal oscillations and equatorial waves" in 2013

Fu, X., B. Wang, D. E. Waliser, and T. Li, 2006: Impact of atmosphere-ocean coupling on the predictability of monsoon intraseasonal oscillations (MISO). J. Atmos. Sci., 64, 157¿174.

Guan, Bin, Duane E. Waliser, Noah P. Molotch, Eric J. Fetzer, Paul J. Neiman, 2012: Does the Madden–Julian Oscillation Influence Wintertime Atmospheric Rivers and Snowpack in the Sierra Nevada?. Mon. Wea. Rev., 140, 325–342. doi: http://dx.doi.org/10.1175/MWR-D-11-00087.1

Hagedorn, R., Buizza, R., Hamill, T. M., Leutbecher, M. and Palmer, T. N. (2012), Comparing TIGGE multimodel forecasts with reforecast-calibrated ECMWF ensemble forecasts. Q.J.R. Meteorol. Soc., 138: 1814–1827. doi: 10.1002/qj.1895

Hanley JA, McNeil BJ. The meaning and use of the area under a Receiver Operating Characteristic (ROC) curve. Radiology, 1982, 143, 29-36.

Hendon, H.H., 2000: Impact of air-sea coupling on the MJO in a GCM. J. Atmos.Sci., 57 , 3939-3952.

Hewitt, H. T., D. Copsey, I. D. Culverwell, C. M. Harris, R. S. R. Hill, A. B. Keen, A. J. McLaren, and E. C. Hunke, 2010, Design and implementation of the infrastructure of HadGEM3: The next generation Met Office climate modelling system. Geosci. Model Dev. Discuss., 3, 1861-1937.

Hoskins BJ, Fonseca R, Blackburn M, Jung T. 2012. Relaxing the Tropics to an 'observed' state: analysis using a simple baroclinic model. Q. J. R. Meteorol. Soc. in press. DOI: 10.1002/qj.1881.

James, P.M., 2007: An objective classification for Hess and Brezowsky. Grosswetterlagen over Europe. Theor. Appl. Climatol., 88, 17-42

Johnson, C. and Swinbank, R. (2009), Medium-range multimodel ensemble combination and calibration. Q.J.R. Meteorol. Soc., 135: 777–794. doi: 10.1002/qj.383

Jolliffe IT, Stephenson DB. (2011)(eds), Forecast Verification: A Practitioner's Guide in Atmospheric Science, Wiley, 274 pages.

Klingaman, N. P. (2013): Improving the MJO in the Hadley Centre climate model: The roles of entrainment and air-sea interactions,
https://ams.confex.com/ams/93Annual/webprogram/Paper222691.html

Klingaman, N.P. and Woolnough, S.J., 2013: Using a case-study approach to improve the Madden-Julian oscillation in the Hadley Centre model. QJRMS: submitted

Lavers, D. A., R. P. Allan, E. F. Wood, G. Villarini, D. J. Brayshaw, and A. J. Wade (2011), Winter floods in Britain are connected to atmospheric rivers, Geophys. Res. Lett., 38, L23803, doi:10.1029/2011GL049783.

Latif, M., M. Collins, H. Pohlmann, N. Keenlyside, 2006: A Review of Predictability Studies of Atlantic Sector Climate on Decadal Time Scales. J. Climate, 19, 5971–5987.
doi: http://dx.doi.org/10.1175/JCLI3945.1

M. Leutbecher, T. N. Palmer , Ensemble forecasting , Journal of Computational Physics - J COMPUT PHYS , vol. 227, no. 7, pp. 3515-3539, 2008. DOI: 10.1016/j.jcp.2007.02.014

Lin, H., Brunet, G., Derome, J., 2009: An Observed Connection between the North Atlantic Oscillation and the Madden–Julian Oscillation. J. Climate, 22, 364–380.
doi: http://dx.doi.org/10.1175/2008JCLI2515.1

Ma, Hsi-Yen, Heng Xiao, C. Roberto Mechoso, Yongkang Xue, 2013: Sensitivity of Global Tropical Climate to Land Surface Processes: Mean State and Interannual Variability. J. Climate, 26, 1818–1837. doi: http://dx.doi.org/10.1175/JCLI-D-12-00142.1

Mason, S. J., 2004: On using "climatology" as a reference strategy in the Brier and ranked probability skill scores. Monthly Weather Review, 137, 1891-1895.

Matsueda, M. and Tanaka, H. L., Can MCGE Outperform the ECMWF Ensemble?
SOLA, 2008, Vol. 4, 077 080, doi:10.2151/sola.2008 02077

Moncrieff, Mitchell W., Duane E. Waliser, Martin J. Miller, Melvyn A. Shapiro, Ghassem R. Asrar, James Caughey, 2012: Multiscale Convective Organization and the YOTC Virtual Global Field Campaign. Bull. Amer. Meteor. Soc., 93, 1171–1187. doi: http://dx.doi.org/10.1175/BAMS-D-11-00233.1

Moore, Richard W., Olivia Martius, Thomas Spengler, 2010: The Modulation of the Subtropical and Extratropical Atmosphere in the Pacific Basin in Response to the Madden–Julian Oscillation. Mon. Wea. Rev., 138, 2761–2779. doi: http://dx.doi.org/10.1175/2010MWR3194.1

Pailleux, J., 1997: 1987-1997, Ten years of research and operational activities with the integrated forecasting system (IFS). ECMWF Newsletter no. 75, Spring 1997.

Palmer, T. N., and Coauthors, 2004: DEVELOPMENT OF A EUROPEAN MULTIMODEL ENSEMBLE SYSTEM FOR SEASONAL-TO-INTERANNUAL PREDICTION (DEMETER). Bull. Amer. Meteor. Soc., 85, 853–872. doi: http://dx.doi.org/10.1175/BAMS-85-6-853

Palmer, T. N., Buizza, R., Doblas-Reyes, F., Jung, T., Leutbecher, M., Shutts, G. J., Steinheimer M., & Weisheimer, A., 2009: Stochastic parametrization and model uncertainty. ECMWF RD TM 598, Shinfield Park, Reading RG2-9AX, UK.

Park, Y.-Y., R. Buizza, and M. Leutbecher, 2008: TIGGE: preliminary results on comparing and combining ensembles. Q. J. R. Meteorol. Soc., 134, 2029-2050 http://www3.interscience.wiley.com/journal/121516300/abstract

Roundy, P., 2011: Tropical–extratropical interactions. Intraseasonal Variability in the Atmosphere-Ocean Climate System, 2nd ed. W. K.-M. Lau and D. E. Waliser, Eds., Springer, 497–512.

Shelly, A., 2013: Predictability and systematic error growth in Met Office MJO ... yotc.ucar.edu/sites/default/files/documents/mjo/events/100615/posters/5j-Shelly_post.pdf (2013.06.19)

Tennant, Warren J., Glenn J. Shutts, Alberto Arribas, Simon A. Thompson, 2011: Using a Stochastic Kinetic Energy Backscatter Scheme to Improve MOGREPS Probabilistic Forecast Skill. Mon. Wea. Rev., 139, 1190–1206.
doi: http://dx.doi.org/10.1175/2010MWR3430.1

Thornes, J.E. and D.B. Stephenson, 2001. How to judge the quality and value of weather forecast products (Meteorol. Appls., 8, 307-314)

Uppala, S. M., KÅllberg, P. W., Simmons, A. J., Andrae, U., Bechtold, V. D. C., Fiorino, M., Gibson, J. K., Haseler, J., Hernandez, A., Kelly, G. A., Li, X., Onogi, K., Saarinen, S., Sokka, N., Allan, R. P., Andersson, E., Arpe, K., Balmaseda, M. A., Beljaars, A. C. M., Berg, L. V. D., Bidlot, J., Bormann, N., Caires, S., Chevallier, F., Dethof, A., Dragosavac, M., Fisher, M., Fuentes, M., Hagemann, S., Hólm, E., Hoskins, B. J., Isaksen, L., Janssen, P. A. E. M., Jenne, R., Mcnally, A. P., Mahfouf, J.-F., Morcrette, J.-J., Rayner, N. A., Saunders, R. W., Simon, P., Sterl, A., Trenberth, K. E., Untch, A., Vasiljevic, D., Viterbo, P. and Woollen, J. (2005), The ERA-40 re-analysis. Q.J.R. Meteorol. Soc., 131: 2961–3012. doi: 10.1256/qj.04.176

Vitart, Frédéric, 2004: Monthly Forecasting at ECMWF. Mon. Wea. Rev., 132, 2761–2779.
doi: http://dx.doi.org/10.1175/MWR2826.1

Vitart, F., Buizza, R., Alonso Balmaseda, M., Balsamo, G., Bidlot, J.-R., Bonet, A., Fuentes, M., Hofstadler, A., Molteni, F. and Palmer, T. N. (2008), The new VarEPS-monthly forecasting system: A first step towards seamless prediction. Q.J.R. Meteorol. Soc., 134: 1789–1799. doi: 10.1002/qj.322

Vitart, F. and Molteni, F. (2010), Simulation of the Madden– Julian Oscillation and its teleconnections in the ECMWF forecast system. Q.J.R. Meteorol. Soc., 136: 842–855. doi: 10.1002/qj.623

Wheeler, M. C. and H. H. Hendon, 2004: An all-season real-time multivariate MJO index: Development of an index for monitoring and prediction. Mon. Wea. Rev., 132, 1917-1932.

Woolnough, S. J., Vitart, F. and Balmaseda, M. A. (2007), The role of the ocean in the Madden–Julian Oscillation: Implications for MJO prediction. Q.J.R. Meteorol. Soc., 133: 117–128. doi: 10.1002/qj.4

Xavier, Prince K., 2012: Intraseasonal Convective Moistening in CMIP3 Models. J. Climate, 25, 2569–2577. doi: http://dx.doi.org/10.1175/JCLI-D-11-00427.1

Zhang, C. (2005), Madden-Julian Oscillation, Rev. Geophys., 43, RG2003, doi:10.1029/2004RG000158.

Zhang, C., M. Dong, H. H. Hendon, E. D. Maloney, A. Marshall, K. R. Sperber, and W. Wang, 2006: Simulations of the Madden-Julian oscillation in four pairs of coupled and uncoupled global models Clim. Dyn. , 27 , 573-592.